Evaluation of a fuzzy-based sliding mode control strategy for a DC-DC buck converter

Quan Vinh Nguyen, Huu-Toan Tran, Long Thang Mai
Faculty of Electronic Technology, Industrial University of Ho Chi Minh City, Ho Chi Minh City, Vietnam

Article Info	ABSTRACT

DC-DC converters operate as semiconductor power devices in which transformers such as buck converters often cause nonlinear characteristics to the converter, while the output voltage of the converter affected by dynamic input voltage and load change. This paper presents a sliding mode control strategy using a fuzzy observer to provide a sustainable response and high performance for buck converters affected by uncertainties such as input voltage and resistance load. The control strategy includes two feedback loops in which an external control loop forces the output voltage to track the set voltage, and the output of the external control loop is adapted as a sliding surface to control the current through the inductor to track the set current, called the internal control loop. Design analysis, control law and Lyapunov stability of the control strategy are illustrated. The simulation is developed on the MATLAB-Simulink platform, the results are re-evaluated experimentally based on the self-built prototype of DC-DC buck converter. The simulated and experimental results have showed that the output voltage and current of the buck converter have tracked the set points from low to high values despite sudden changes in load as well as in input voltage in the presence of noise. The compatibility index normalized root mean square error of the measured voltage and current using the proposed algorithm is [96.34%±1.02%, 95.09%±3.04%] higher than that using the proportional integral (PI) algorithm which is [95.94% ± 3.01%, 85.72% ± 3.95%] in the presence of varying parameters.

Corresponding Author:

Huu-Toan Tran
Faculty of Electronic Technology, Industrial University of Ho Chi Minh City
Ho Chi Minh City, Vietnam
Email: tranhuutoan@iuh.edu.vn

1. INTRODUCTION

Voltage control and current control are two commonly used methods to control DC-DC converters [1], [2]. Voltage control has a significant ability to reject noise yet has slow time-response while, as a trade-off, current control is a fast transient response method yet more complicated than the voltage control. Classical proportional integral (PI) controllers using carrier wave and hysteretic controllers are most commonly utilized for DC-DC converters [3], [4]. Classical controllers are simply implemented but affected by the influences of uncertain parameters existing in the converter, thus, are not very effective in achieving the desired performance [5], [6]. The controllers of a DC-DC converter have to take into account nonlinearities and parameter variations of the converter in order to guarantee global stability and provide fast time-response under all conditions [7], [8].

In order to improve the control performance of the classical controllers, artificial neural networks (ANN) is trained using approximation dynamic programming (ADP) to allow optimal control with the inputs of error signals and integrals of the error signals [9], [10]. Optimization algorithms such as particle swarm

optimization (PSO) are utilized to select PI parameters and to address the wind-up issue of the buck converter control [11], [12]. In order to generate the desired voltage with high robustness to load disturbances, a parametric function approximator is proposed to provide optimal switching for the converter [13]. A nonlinear control technique derived from the concept of variable structure control called sliding mode control (SMC) which has the advantages of simple implementation, robust stability and fast time-response [14]. SMC is adopted for DC-DC buck converter to provide a stable constant output voltage that counteracts the effect of uncertainties such as input voltage and resistance load [15]. The chattering phenomena are unexpected oscillations of finite amplitude and frequency due to the presence of un-modeled dynamics or discrete-time implementation [16]. In order to improve the performance of SMC, equivalent control and boundary layer approach control are proposed to reduce noise yet cannot reduce chattering phenomena due to their finite number of output values. The approach of boundary layer asymptote encountered in reaching the sliding mode due to replacing the discontinuous function sign(.) with the continuous saturation function Sat(.) [17]-[20].

A fuzzy set is a mathematical soft-computing model constructed by heuristic information from human reasoning process that provides an efficient methodology for implementing a human's heuristic knowledge about how to observe, identify, and control a system [21], [22]. The fuzzy controller commonly operated as a supervisor, a gain scheduling, an adaptive regulator, or a robust stability term [23]-[25]. Analytical methods are not amenable to nonlinear, time-varying, or unknown infinite-dimensional systems which are able to be handled using fuzzy controllers [26]-[30]. In this paper, a new fuzzy-based sliding mode control strategy (FSMCS) for the DC-DC buck converter is proposed to reduce the effects of chattering phenomena and uncertainties. The combination of the sliding mode control (SMC) and fuzzy logic provides a significant solution as a supervisor to tune the sliding mode output. In FSMCS, the fuzzy system is utilized to estimate the upper limits of noise and uncertainties to reduce the chattering behavior. The advantage of FSMCS is that the control law is not directly extracted from the mathematical model of the controlled system [31]-[34]. The model of buck converters affected by uncertainties such as input voltage and load resistance is shown. The sliding control law and the fuzzy observer are designed to provide a sustainable response and high performance for the buck converters. The FSMCS is composed of external and internal control loops. The external control loop is to force the output voltage to track the set voltage when the output of the external control loop is adapted as a sliding surface to control the current through the inductor to obtain the set current. A fuzzy supervisor is proposed for the sliding surface to generate PWM pulses that have efficient duty cycles for the buck converter's switch to provide a stable, constant output voltage. Stability analysis of the control system is proved using Lyapunov theory. The proposed strategy was evaluated on both simulated and experimental platforms using MATLAB Simulink and 320F28379 DSP Card. The simulated and experimental results have shown that the output voltage and current of the buck converter have tracked the set points from low to high values despite sudden changes in load as well as in input voltage in the presence of noise.

The remainder of this paper is organized as follows: i) Firstly, a mathematical model for DC–DC converter is presented, and the design of the FSMCS control law is drawn; ii) Subsequently, we discuss how the fuzzy is designed and the controlled system is stable; and iii) Finally, simulations and experiments are implemented to validate the feasibility of the proposed FSMCS.

2. FUZZY-BASED SLIDING MODE CONTROL STRATEGY (FSMCS) FOR THE DC-DC BUCK CONVERTER

In this section, the solid DC-DC buck converter model is presented to produce the control law principle. The proposed fuzzy-based sliding mode control strategy includes two feedback loops in which an external control loop forces the output voltage to track the set voltage, and the output of the external control loop is adapted as a sliding surface to control the current through the inductor to track the set current. Design analysis, control law, and Lyapunov stability of the control strategy are illustrated.

2.1. DC-DC buck converter model

Figure 1 shows a traditional DC-DC buck converter schematic in which the output voltage of the converter V_O is lower than the input supply voltage V_{In}. This is achieved by periodically opening and closing the switching element in the power switching circuit. When the switch is in the ON position, the circuit is connected to the input source V_{In} creates an output voltage V_O across the load resistor. If the switch is turned to the OFF position, the voltage across the capacitor will discharge through the load. The switch position controls the output voltage V_O which can be maintained at a desired level below the input supply voltage V_{In}.

The Buck converter can be described by the following differential equations:

$$\begin{cases} \frac{dI_L(t)}{dt} = \frac{V_{In}}{L}u(t) - \frac{V_O(t)}{L} \\ \frac{dV_O(t)}{dt} = \frac{I_L(t)}{C} - \frac{V_O(t)}{R_L C} \end{cases} \tag{1}$$

where $u(t)$ is the discontinuous control input, $I_L(t)$ is the current passing through the inductor L, the control objective is such that the voltage on the load $V_O(t)$ follows the setting voltage V_O^* in the presence of the uncertainties in the resistance load R_L and input voltage V_{In}.

The (1) can be converted into state space form as (2).

$$\begin{bmatrix} \frac{dx_1(t)}{dt} \\ \frac{dx_2(t)}{dt} \end{bmatrix} = \begin{bmatrix} 0 & 1 \\ -\frac{1}{LC} & \frac{1}{R_LC} \end{bmatrix} \begin{bmatrix} x_1(t) \\ x_2(t) \end{bmatrix} + \begin{bmatrix} 0 \\ -\frac{V_{In}}{R_LC} \end{bmatrix} u(t) + \begin{bmatrix} 0 \\ \frac{V_O^*(t)}{LC} \end{bmatrix} \tag{2}$$

The control input and state space variables are given as (3), (4), and (5).

$$u(t) = \begin{cases} 1, & while\ S = On \\ 0, & while\ S = Off \end{cases} \tag{3}$$

$$x_1(t) = V_O^*(t) - V_O(t) \tag{4}$$

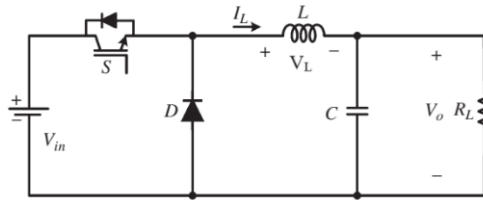$$x_2(t) = \frac{dx_1(t)}{dt} = \frac{dV_O^*(t)}{dt} - \frac{dV_O(t)}{dt} \tag{5}$$

Figure 1. DC-DC buck converter

2.2. FSMCS design

A new fuzzy-based sliding mode control strategy including two feedback loops is proposed in which an external control loop to force the output voltage to track the set voltage, and the output of the external control loop is adapted as a sliding surface to control the current through the inductor to track the set current, called the internal control loop, as depicted in Figure 2. The control law $u(t)$ will change the duty cycle, in which the outer loop controller given by (6) forces the voltage on the load $V_O(t)$ tracks to the setting voltage $V_O^*(t)$. On the other hand, the inner loop controller yields the input load current $I_L(t)$ that tracks the current setting $I_L^*(t)$ to reduce consumption for the converter.

$$I_L^*(t) = K_P\left(\frac{dV_O^*(t)}{dt} - \frac{dV_O(t)}{dt}\right) + K_I \int \left(\frac{dV_O^*(t)}{dt} - \frac{dV_O(t)}{dt}\right) dt \tag{6}$$
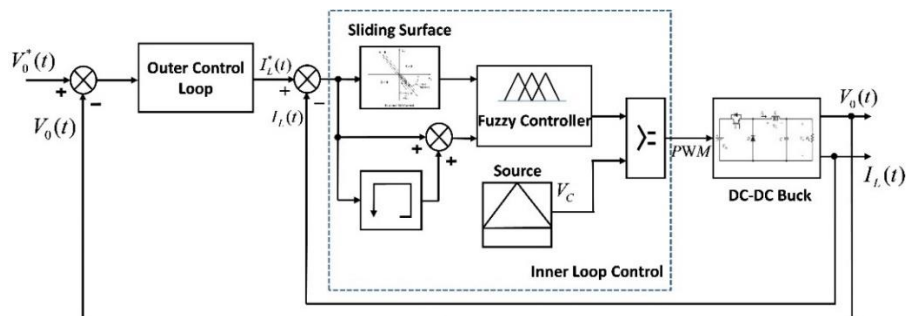

Figure 2. Diagram of the proposed FSMCS for a buck converter

The pulse width modulation (PWM) obtained by comparing the control law $u(t)$ with the triangular carrier wave $V_C(t)$. The duty cycle coefficient N is calculated as (7), defining the switching frequency as shown in (8).

$$N = \frac{T_{On}}{T} \tag{7}$$

$$f_{sw} = \frac{1}{T} = \frac{1}{T_{On} + T_{Off}} \tag{8}$$

2.3. SMC design

Considering an autonom system with input signal $u(t) = [u_1(t), u_2(t), \ldots, u_m(t)]$, uncertainty and noise components $d(t, x(t), u(t))$ is described by a state space form as (9):

$$\frac{dx(t)}{dt} = f(t, x(t), u(t), d), \tag{9}$$

where $x \in R^n$ is the state vector, $f(.) \in R^n$ is the vector of continuous functions and $u \in R^m$ is the control input vector. A smooth curved surface called a sliding surface is described as (10).

$$s(x) = c_1 e(t) = c_1(I_L^* - I_L), c_1 > 0 \tag{10}$$

The function of the sliding control is to determine the control law $u(t)$ to bring the system (9) towards the sliding surface (10) and to retain it on the surface, that is, so that the state vector $I_L(t)$ tracks to a desired trajectory $I_L^*(t)$ given by (6).

The derivative of the sliding surface according to the classical proportionality law is (11).

$$\frac{ds}{dt} = -\eta \, sgn(s), \ \eta > 0 \tag{11}$$

The sign function $sgn(.)$ has the formula given in (12).

$$sgn(s) = \begin{cases} -1, & \text{if } s < 0 \\ 0, & \text{if } s = 0 \\ 1, & \text{if } s > 0 \end{cases} \tag{12}$$

A positive function is chosen as (13):

$$L = \frac{1}{2} s^T s \tag{13}$$

to ensure that the state trajectory approaches and slides on the sliding surface, the stability condition (14) has to be satisfied as (14).

$$\frac{dL}{dt} = s^T \dot{s} \le 0 \tag{14}$$

After substituting (11) into (14), the Lyapunov stability is obtained:

$$\frac{dL}{dt} = -\eta s \, sgn(s) = -\eta |s| \le 0 \tag{15}$$

where η is a positive constant that ensures the system's trajectory approaches the sliding surface in a finite time. This is also a sufficient condition for the control signal to bring the system's state trajectory $x(t)$ back to the sliding surface.

Substituting (6), (10) into (14), the stability condition for the DC-DC buck converter is obtained such that the following inequality holds:

$$V_O(t) \le V_{In} \tag{16}$$

therefore, for a DC-DC buck converter, the output voltage must be less than the supply voltage to assure a sliding control implementation.

2.4. Fuzzy observer design

In reality, the ideal sign function defined by (12) does not exist, instead the following function is significantly utilized:

$$sgn(s) = \begin{cases} -1, & \text{if } s < -\varepsilon \\ previous \ state, & \text{if } |s| \le \varepsilon \\ 1, & \text{if } s > \varepsilon \end{cases} \tag{17}$$

This choice causes the chattering phenomena in the system, where the function must change sign with extremely high frequency to keep $x(t)$ on the sliding surface $s(x) = 0$.

The sliding mode control principle is shown in Figure 3, where $s(x) = 0$ represents the sliding surface and $x_1(t)$, $x_2(t)$ are the voltage (or current) error and its derivative, respectively. The sliding line divides the phase plane into two regions who's each one is identified by a switching state. When the trajectory reaches the system's equilibrium point, the system is stable [25].

If the delay range around the sliding line is zero then the system is operated with ideal sliding mode control as shown in Figure 3(a). However, in practical terms this ideal control is not achievable. Therefore, the actual sliding mode control operation is that the non-ideal delay range has a finite switching frequency as shown in Figure 3(b). To minimize the chattering behavior and increase the performance of the sliding mode controller, a fuzzy observer is proposed to adjust the delay range of the sliding surface as desired in which function $f = \eta \, sgn(s)$ will be approximated by the fuzzy system called $\hat{f}$.
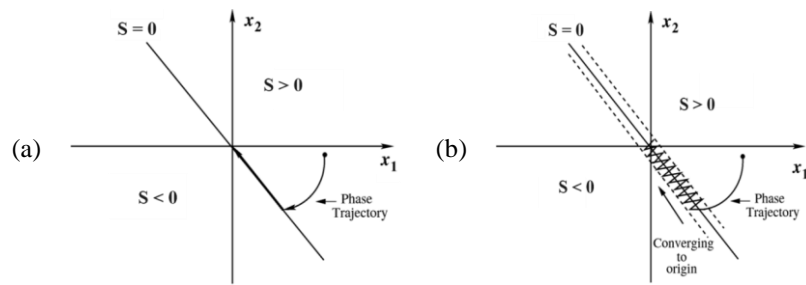

Figure 3. Phase plot for sliding mode control: (a) ideal SM control and (b) actual SM control

Fuzzy logic is a theory of fuzzy sets based on a linguistic description rather than a mathematical model of a system. This logic provides an efficient tool to apply heuristic knowledge of an experienced operator or an expert to control the system with non-model problems. In the proposed fuzzy-based sliding mode control strategy, the fuzzy plays a role as a supervisor to tune the duty cycle coefficient N based on the observation of the sliding mode output.

The input signals of the proposed fuzzy-based regulator are the outputs of the outer loop controller:

$$x = \begin{bmatrix} e(t) & \dfrac{de(t)}{dt} \end{bmatrix}^T \tag{18}$$

where $e(t) = I_L^*(t) - I_L(t)$ is the current error between the desired current $I_L^*(t)$ and the measured current $I_L(t)$. The inputs $x = \begin{bmatrix} e(t) & \frac{de(t)}{dt} \end{bmatrix}$ are normalized within $[-1 \quad 1]$ by scaling factors K_E, K_{DE}, respectively. K_E is chosen as $min\{1/|e_{max}|||e_{min}|||\}$ and K_{DE} is set equal to $min\{1/|de_{max}|||de_{min}|||\}$. A scaling factor K_N is also added for fuzzy output to obtain an actual duty cycle.

$$\mu_{NM}(x) = e^{-\left(\frac{x+\frac{\pi}{6}}{\frac{\pi}{24}}\right)^2} ; \mu_{NS}(x) = e^{-\left(\frac{x+\frac{\pi}{12}}{\frac{\pi}{24}}\right)^2} ;$$
$$\mu_{ZO}(x) = e^{-\left(\frac{x}{\pi/24}\right)^2} ; \mu_{PS}(x) = e^{-\left(\frac{x-\pi/12}{\pi/24}\right)^2} ; \mu_{PM}(x) = e^{-\left(\frac{x-\pi/6}{\pi/24}\right)^2} \tag{19}$$

The designed fuzzy system consists of a fuzzification stage, a rule-based inference mechanism and a defuzzification stage [26]. Five Gaussian membership functions are defined {negative medium (NM), negative small (NS), zero (ZO), positive small (PS), positive medium (PM)} for each input variable while five Gaussian membership functions are similarly defined for the output variable. The (19) expresses the parameterized Gaussian membership function for the fuzzy design.

The fuzzy rule base is inferred based on linguistic values of the input variables, as described in Table 1. The rules are identified based on the following functional characteristics and analyses for the converter control performance:
- In cases where the converter output is significantly deviated from the set point value, the duty cycle N must be large to bring the output to the set point quickly.
- If the converter output trends gradually toward the set point value, the duty cycle N changes should be insignificant compared to its current value.

- In cases where the converter output is toward the set point value with high velocity, the duty cycle N should not be changed to avoid the overshoot phenomenon.
- If the converter output reaches the set point value stably, duty cycle N should not be changed.
- In cases the converter output is higher than the set point, the change sign of N has to be negative and vice versa.

The center of gravity method was utilized for defuzzification as mentioned in (20), where S = {y $\in$ Y|μ$_R$(y) > 0} is the specified domain of the fuzzy set μ$_R$(y).

$$y_O = \frac{\int_S y \mu_R(y) dy}{\int_S \mu_R(y) dy} \qquad (20)$$

The characteristic surface of fuzzy model shown in Figure 4 demonstrates the effects of $e(t)$ and $de(t)/dt$ on the output of the fuzzy system. The output increases rapidly when $e(t)$ increases from -1 to $+1$. In cases where $de(t)/dt$ increases from -1 to $+1$, the output is correspondingly reduced. Therefore, the error $e(t)$ and its derivate $de(t)/dt$ will affect the control performance for the converter over the entire operating range.

Table 1. Fuzzy rule base for FSMCS

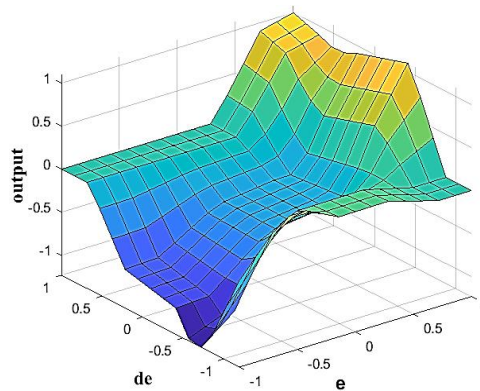| de | e	NM	NS	ZO	PS	PM
NM	NM	NM	NM	NS	ZO
NS	NM	NM	NS	ZO	PS
ZO	NM	NS	ZO	PS	PM
PS	NS	ZO	PS	PM	PM
PM	ZO	PS	PM	PM	PM

Figure 4. Surface view of the designed fuzzy system

3.   EVALUATION OF THE PROPOSED ALGORITHM IN SIMULATION AND EXPERIMENT

In this work, a preliminary evaluation of the combined fuzzy-sliding approach has been performed on both simulated and real systems. The simulated models have been re-evaluated on our custom-built real-time system. Simulations and experiments were performed on MATLAB/Simulink with sampling time, the converter parameters are given in Table 2.

Table 2. Simulated and experimental parameters of the converter

Parameters	Values	Parameters	Values
V_{In}	90 (V)	K_P, K_I	0.5, 20
V_O^*	50 (V)	D_{max}	10 (V)
L, C, R_L	100 (μH), 680 (μF), 10 (Ω)	$T_S T_S$	10 (μs)
f_C	10 (KHz)		

3.1. Simulation results

Figure 2 also shows the corresponding Simulink diagram of the DC-DC buck converter control using FSMCS with the sampling time $T_S = 10\ \mu s$. The control goal is to implement the sliding mode control algorithm with a fuzzy observer that identifies the changes in the function $f = \eta\ sgn(s)$ to reduce the chattering behavior and to improve the robustness of the controller in the cases of load change and high dynamic performance (e.g., rising response-time and overshoot, limited output harmonic, and so on). The

control strategy is demonstrated in the presence of input voltage changes and random distribution noise $d(t)$. The performance of the DC-DC buck converter control is validated under four different conditions, which are instantaneous change at the initial condition, change in the supply voltage V_{In}, change in RL loads, and unpredictable changes in uncertainties of the converter circuit.

The simulation results present the control response of the output voltage and current through the inductor L for both the FSMCS control and PI control cases when the quantities V_O^*, V_{In}, and R_L change suddenly. In all simulated and experimental results, the black line is the DC power supply V_{In}, the dashed red lines are the set values V_O^*, I_L^* and the solid blue lines are the measured values V_O, I_L. To quantitatively compare between the classical PI control and the proposed FSMCS, the performance index normalized root mean square error (NRMSE), is defined as (21). The NRMSE represents the degree of compatibility between the setting signal y^* and the measured signal y in which mean(y) is the average value of y.

$$NRMSE = 100\left(1 - \frac{\|y^*-y\|}{\|y^*-mean(y^*)\|}\right) \tag{21}$$

Figure 5(a) presents the control response using FSMCS in case the voltage $V_{In} = 90\,V$ shows that the measured voltage V_O and the measured current I_L ensure tracking performance to the set values V_O^* and I_L^* with various levels. Because the average value of current through the capacitor C is zero, the highest value of current $I_L = \frac{V_O}{RL} = 5\,A$. However, as seen in Figure 5(b), the current I_L is instantaneously overshoots at the initial condition with PI control. Moreover, the compatibility level of the measured voltage V_O and current I_L using the FSMCS algorithm is NRMSE = [96.34%, 92.05%] higher than that using the PI algorithm, which is NRMSE = [95.94%, 88.99%]. Figure 6 shows simulation results when a sudden change in voltage V_{In} from 90 V to 60 V is fed at 0.5 seconds.

As expected, voltage V_O and current I_L with FSMCS control, track the setting values V_O^* and I_L^* that are not affected by the change (Figure 6(a)) compared to the PI control (Figure 6(b)). The current I_L does not change because the output voltage does not change and has the highest value $I_L^* = \frac{V_O^*}{RL} = 5\,A$. The PI control result, as shown in Figure 6(b) shows a voltage drop of about 3 V and a current overshoot of 0.7 A before returning to equilibrium after a period of 0.1 seconds. The compatibility level of the measured voltage V_O and measured the current I_L using the FSMCS algorithm is NRMSE = [96.42%, 93.48%] higher than in the case using the PI algorithm, which is NRMSE = [95.88%, 85.72%]. Figure 7 shows simulation results when the load R_L suddenly changes from 10 Ω to 5 Ω under the condition $V_{In} = 90\,V$ at 3.5 seconds. Despite the sudden change of R_L, the proposed controller still forces the measured voltage V_O and current I_L to track the setting values V_O^* and I_L^* in which the voltage drops about 5 V in an insignificant time then returns to the initially stable state. For PI control, the overshoot of the measured current I_L arose at instants that V_O^* changes rapidly. This demonstrated that the changes of parameters are yet conducted by a simple PI controller. Similarly, to the case of the voltage V_{In} change, the compatibility level of V_O and $I_L I_L$ using the FSMCS algorithm is NRMSE = [95.82%, 93.97%] higher than in the case using PI algorithm, which is NRMSE = [95.44%, 91.92%].
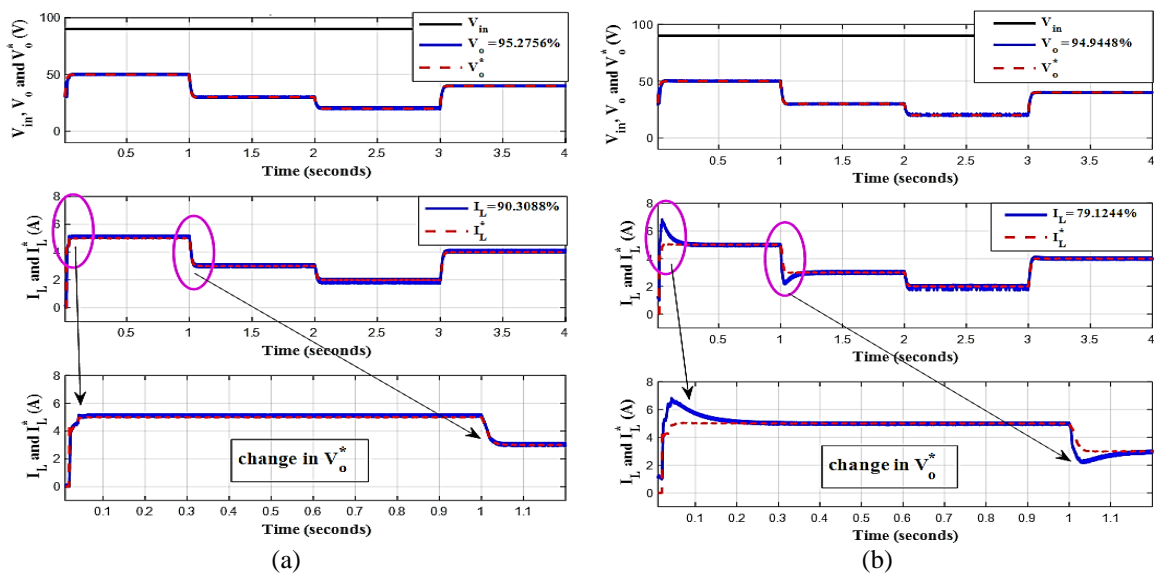

Figure 5. Control response V_o and I_L in the case $V_{in} = 90$ V: (a) FSM control and (b) PI control
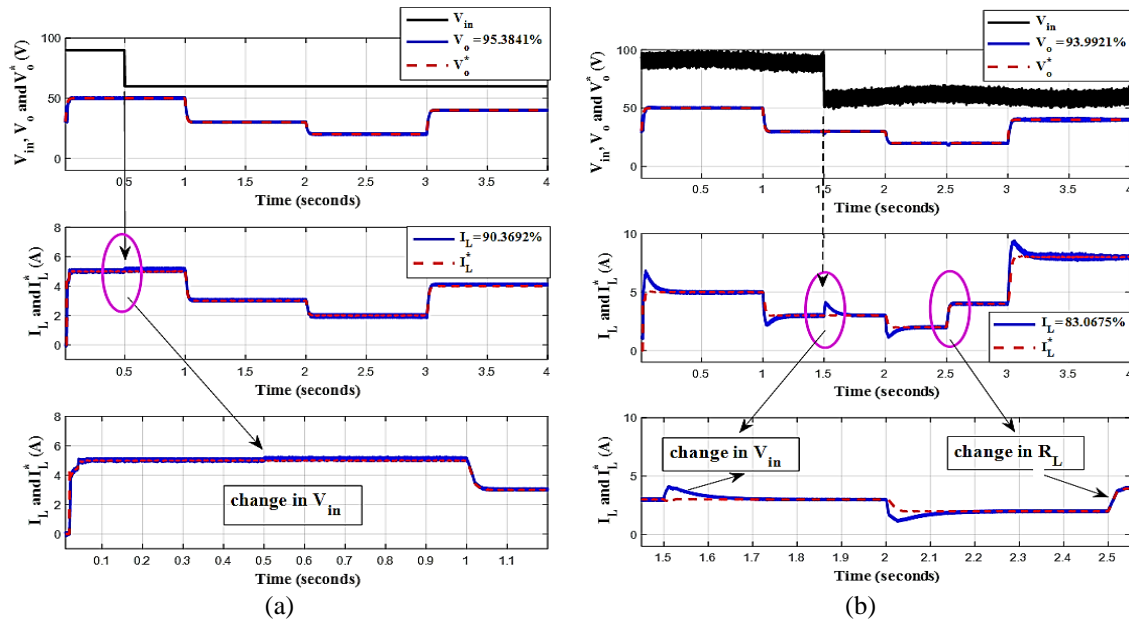
Figure 6. Control response V_o and I_L in the case V_{in} changed at 0.5 seconds:
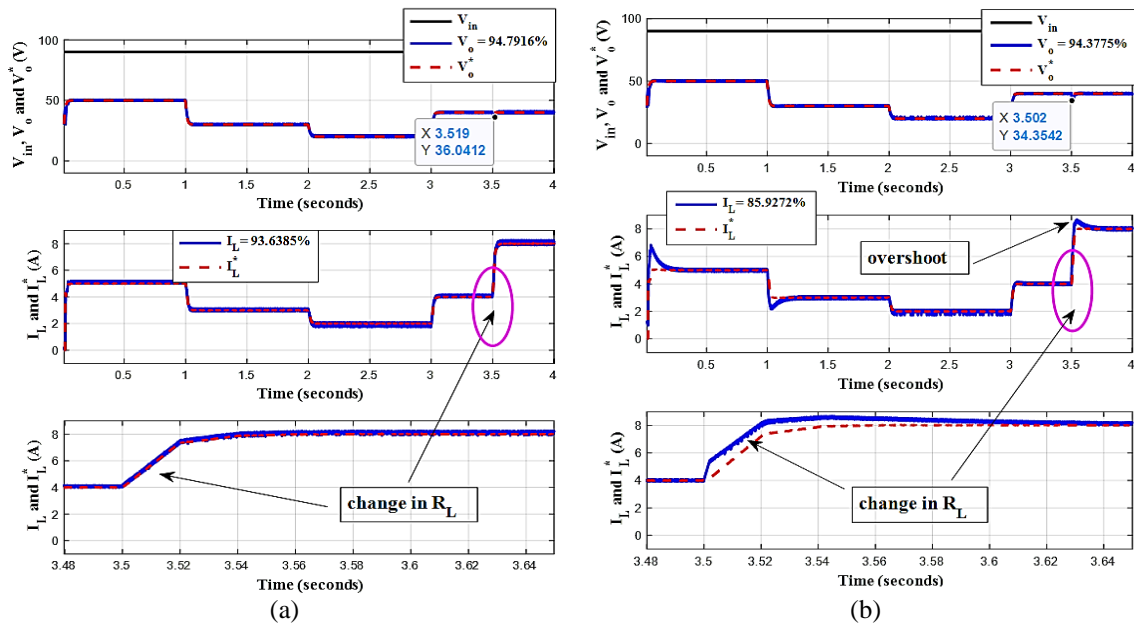(a) FSM control and (b) PI control

Figure 7. Control response V_o and I_L in the case R_L changed at 3.5 seconds: (a) FSM control and (b) PI control

In the case when V_{In}, V_O^*, and R_L change simultaneously, Figure 8 shows that the measured voltage V_O and current I_L still to track the setting values with much higher-quality control performance. The FSMCS controller is not significantly affected, while the PI controller is still very sensitive to parameter variations, in which the overshoot of the measured current I_L significantly arose at instants that V_O^* changes rapidly. The compatibility level of V_O and I_L using the FSMC algorithm is NRMSE = [95.88%, 94.98%] higher than in the case using PI algorithm is NRMSE = [95.37%, 89.67%].

Figure 9 shows simulation results when a noise $d(t)$ is fed into V_{In} along with changes in V_O^* and R_L. As expected, the measured voltage V_O and current I_L with FSMCS control track the setting values V_O^* and I_L^* that are not affected by noise (Figure 9(a)) compared to the PI control (Figure 9(b)). The compatibility level of V_O and I_L using the FSMCS algorithm is NRMSE = [95.92%, 95.09%] still higher than the case using PI algorithm is NRMSE = [92.39%, 89.64%].
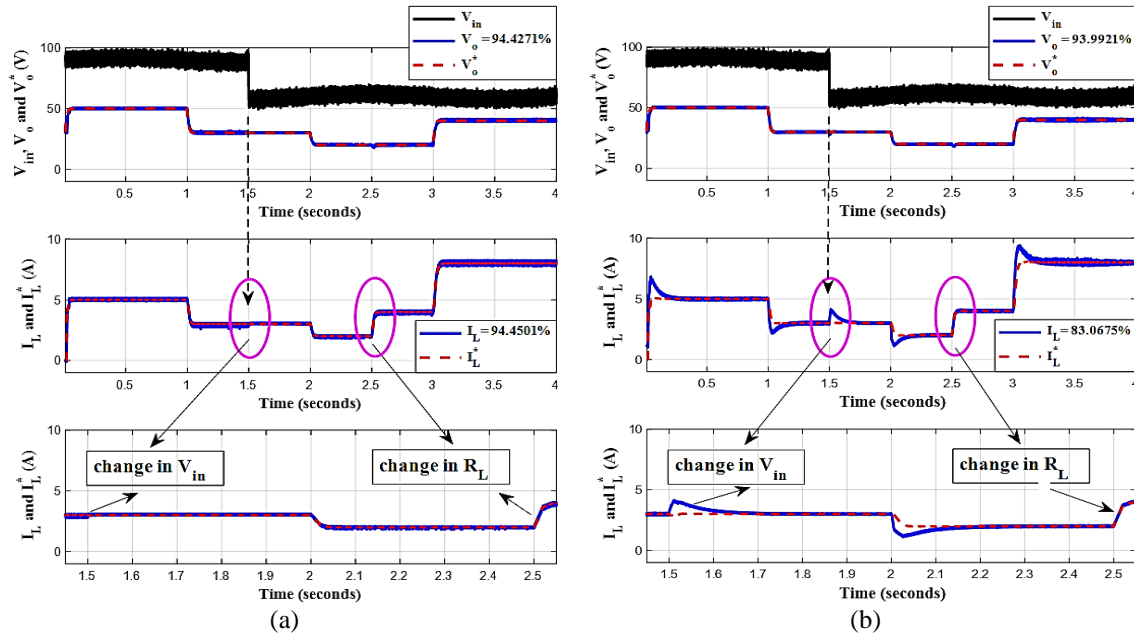
Figure 8. Control response V_o and I_L in the case where V_{in} and R_L are both changed:
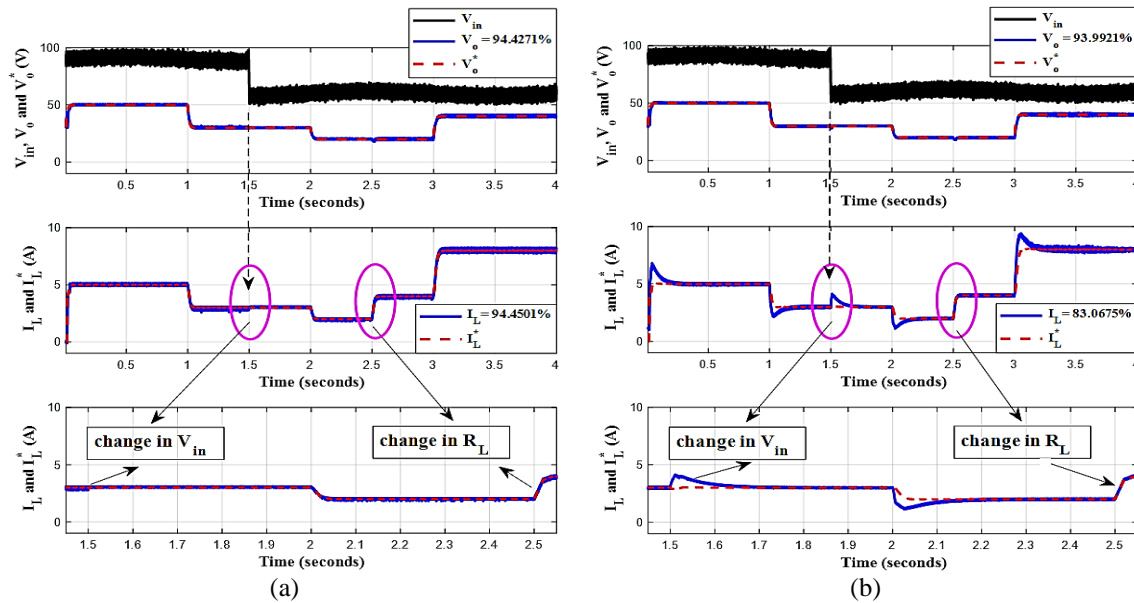(a) FSM control and (b) PI control

Figure 9. Control responses V_o and I_L in the case noise distribution $d(t)$ is fed:
(a) FSM control and (b) PI control

Figure 10 shows $\frac{dL}{dt} = s^T \dot{s} \leq 0$ despite the sudden changes of V_O^*, V_{In}, and R_L in the presence of the noise. The FSMCS algorithm satisfies the Lyapunov stability condition (14), so the stability of the buck converter against such disturbances is guaranteed. Simulation results demonstrated that the proposed FSMCS algorithm is an advanced control method for the DC-DC buck converter, the output voltage of the buck converter has tracked various setting points despite sudden changes in the source input, load as well as the presence of noise. The improved control quality indexes include rapid recovery time in the presence of varying parameters, insignificant steady-state error, small overshoot, and high degree of compatibility of the measured voltage V_O and current I_L compared to the classical PI controller. Table 3 presents a summary comparison of compatibility of the measured voltage V_O and current I_L between FSMCS and PI control algorithms which shows that the FSMCS is more performance efficient with higher NRMSE coefficients.
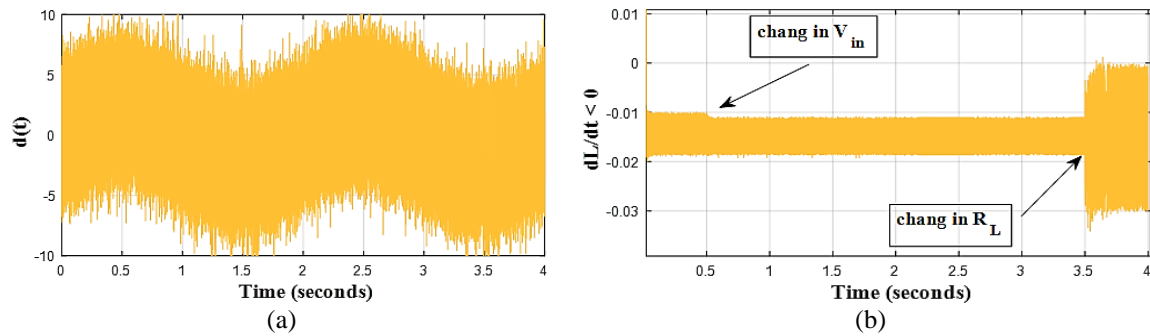
Figure 10. Response of Lyapunov stability condition in the case noise d(t) is fed:
(a) random noise distribution $d(t)$ and (b) performance $\frac{dL}{dt} = s^T \dot{s} \leq 0$

Table 3. The comparison of NRMSE coefficients

V_{in}, V^*_o, and R_L	FSMC	PI
V_{in} = 90 V	[96.34%, 92.05%]	[95.94%, 88.99%]
Change in V_{in}	[96.42%, 93.48%]	[95.88%, 85.72%]
Change in R_L	[95.82%, 93.97%]	[95.44%, 91.92%]
Change V_{in}, R_L	[95.88%, 94.98%]	[95.37%, 89.67%]
Change in d(t)	[95.92%, 95.09%]	[95.39%, 89.64%]

3.2. Experimental results

In this work, a real-time experimental model is built for a DC-DC buck converter circuit with sampling time Ts = 10 μs as depicted in Figure 11. The architecture of the experimental setup includes a custom-built DC-DC buck converter, an oscillator and a LCD Monitor for signal measurement and visual feedback, an user interface and control program with MATLAB/Simulink on a PC. The DC-DC buck converter circuit communicates with the control center via a PCI card to provide an understandable and consistent behavior and comfortable data visualization. The evaluations were carried out at Faculty of Electronics Technology (FET) with the approval of Industrial University of Ho Chi Minh City. The model parameters are also given in Table 2. The control program is implemented on MATLAB/Simulink which the experimental response of the converter is collected on a computer via DSP card 320F28379 and the setting voltage V_O^* is adjusted by a 1 KΩ fine-tuning potentiometer.

Figure 12 presents the experimental control response using FSMCS in case the voltage $V_{In} = 90\ V$ shows that the measured voltage V_O and the measured current I_L track to the setting values V_O^* and I_L^* with high quality performance. For PI control, the current I_L is instantaneously overshoot at initial condition as seen in Figure 9(b). The compatibility level of the measured voltage V_O and current I_L using the FSMCS algorithm is NRMSE = [95.72%, 90.99%] higher than that using the PI algorithm which is NRMSE = [95.21%, 84.22%].
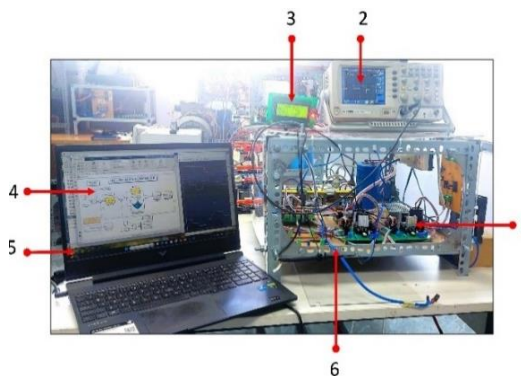

Figure 11. The experimental setup used in this paper was developed at the Industrial University of Ho Chi Minh City: 1) a custom-built DC-DC buck converter, 2) Oscillator for signal measurement, 3) LCD Monitor for visual feedback, 4) user interface and Control program, 5) PC with MATLAB/Simulink for control & data acquisition, and 6) testing-bench
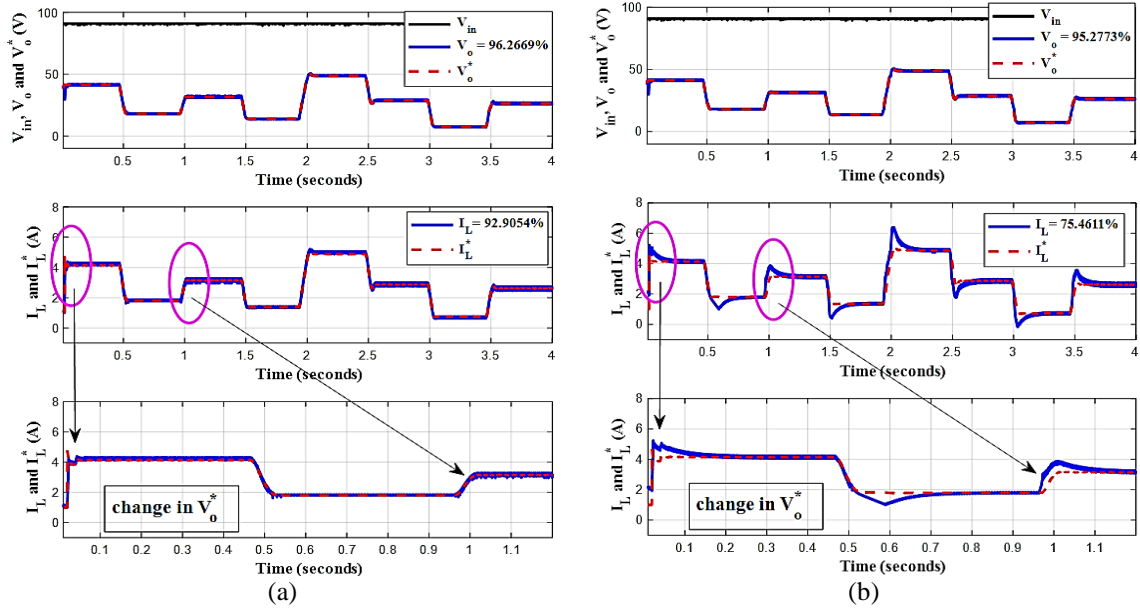
Figure 12. Experimental control response in the case V_{in} = 90 V: (a) FSM control and (b) PI control

Figure 13 shows experimental results when a sudden change in voltage V_{In} from 90 to 60 V appear at 1.25 seconds. The measured voltage V_O and current I_L with FSMCS control, track the setting values V_O^* and I_L^* that are not affected by the change as seen in Figure 13(a). The current I_L does not change and has the highest value $I_L^* = \frac{V_O^*}{RL} = 5\,A$. However, the overshoot of the current I_L arose at instant when V_O^* changes rapidly in the case using the PI control as seen in Figure 13(b). Similarly, to the simulation results, the compatibility level of the measured voltage V_O and measured the current I_L using the FSMCS an algorithm is NRMSE = [95.59%, 91.75%] higher than in the case using the PI algorithm, which is NRMSE = [94.91%, 78.06%].
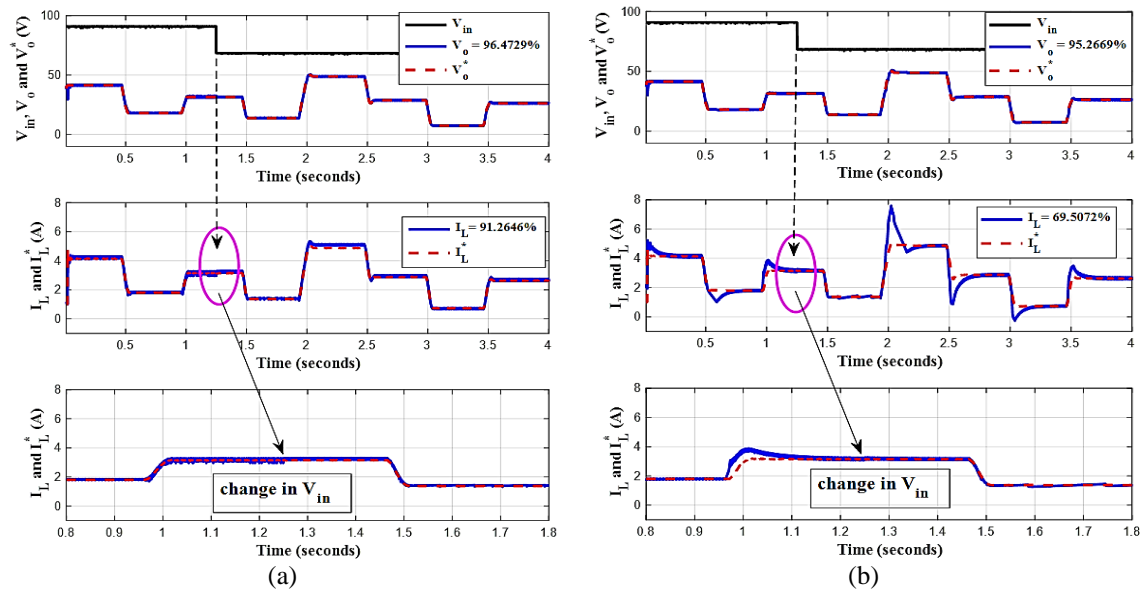

Figure 13. Experimental control response V_o and I_L in the case V_{in} changed at 1.25 seconds:
(a) FSM control and (b) PI control

Figure 14 shows experimental results when the load R_L suddenly changes from 10 Ω to 5 Ω under the condition $V_{In} = 90\,V$ at 2.25 seconds. Despite the sudden change of R_L, the proposed controller still

forces the measured voltage V_O and current I_L to track the setting values V_O^* and I_L^* in which the voltage drops about 7 V in an insignificant time then returns to the initially stable state. For PI control, the overshoot of measured current I_L is about 0.6 A at instants that V_O^* changes rapidly. Similarly, to the case of simulation, the compatibility level of V_O and I_L using the FSMCS algorithm is NRMSE = [94.15%, 93.75%] higher than in the case using PI algorithm which is NRMSE = [93.69%, 89.37%].

In the case when V_{In}, V_O^*, and R_L change simultaneously, Figure 15(a) shows that the measured voltage V_O and current I_L using FSMCS, track the setting values significantly. Whereas the PI controller is significantly affected by parameter variations, in which the overshoot of the measured current I_L appears at instants that V_O^* changes rapidly as shown in Figure 15(b). The compatibility level of V_O and I_L using the FSMC algorithm NRMSE is = [93.89%, 94.00%] higher than in the case using PI algorithm is NRMSE = [93.45%, 86.26%].
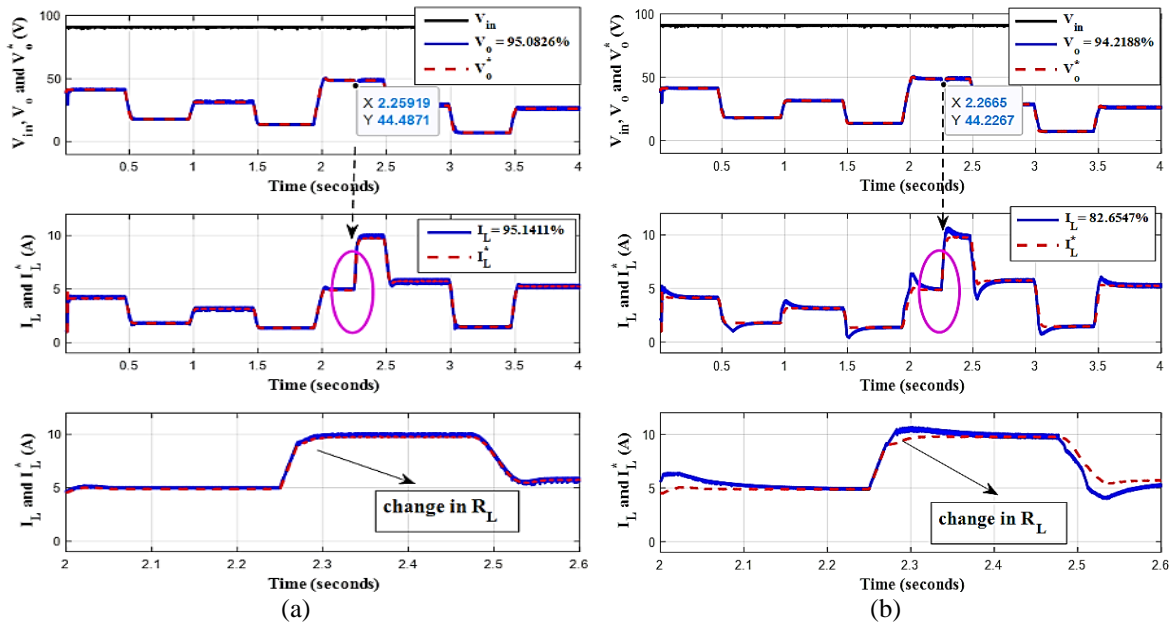

Figure 14. Experimental control response V_o and I_L in the case R_L changed at 2.25 seconds:
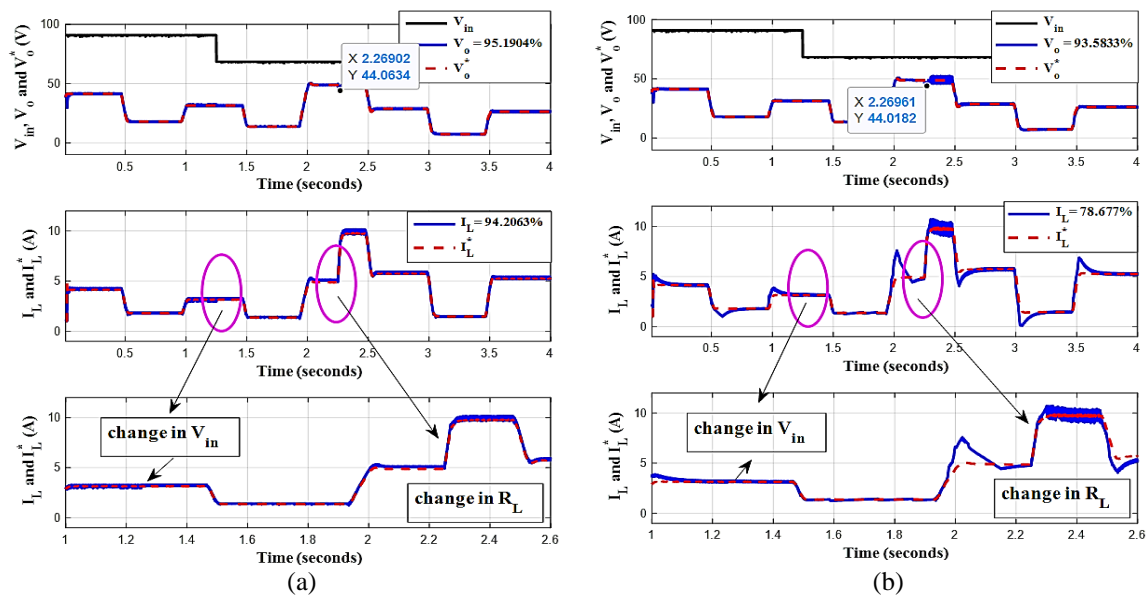(a) FSM control and (b) PI control

Figure 15. Experimental control response V_o and I_L in the case where V_{in} and R_L are both changed:
(a) FSM control and (b) PI control

Figure 16 shows experimental results when a noise $d(t)$ appeared in V_{In} along with changes in V_O^* and R_L. As expected, the measured voltage V_O and current I_L using FSMCS control track the setting values V_O^* and I_L^* that are not affected by noise (Figure 16(a)) compared to the case using PI control (Figure 16(b)). The compatibility level of V_O and I_L using the FSMCS algorithm is NRMSE = [93.94%, 94.20%] still higher than the case using PI algorithm is NRMSE = [93.41%, 86.27%].

Figure 17(a) shows the random noise distribution $d(t)$ with amplitude ±10 V appeared in control procedure while Figure 17(b) shows $\frac{dL}{dt} = s^T \dot{s} \leq 0$ despite the sudden changes of V_O^*, V_{In}, and R_L in the presence of the noise. The experimental results also demonstrated that the stability of the buck converter against such disturbances is guaranteed since the FSMCS algorithm satisfies the Lyapunov stability condition.
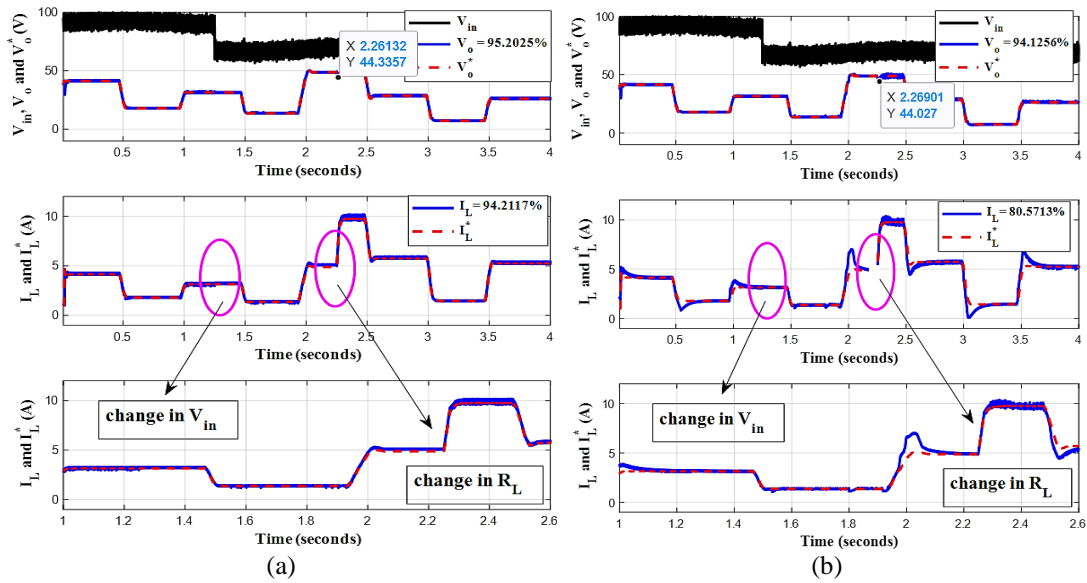

Figure 16. Experimental control responses V_o and I_L in the case noise distribution $d(t)$ appeared:
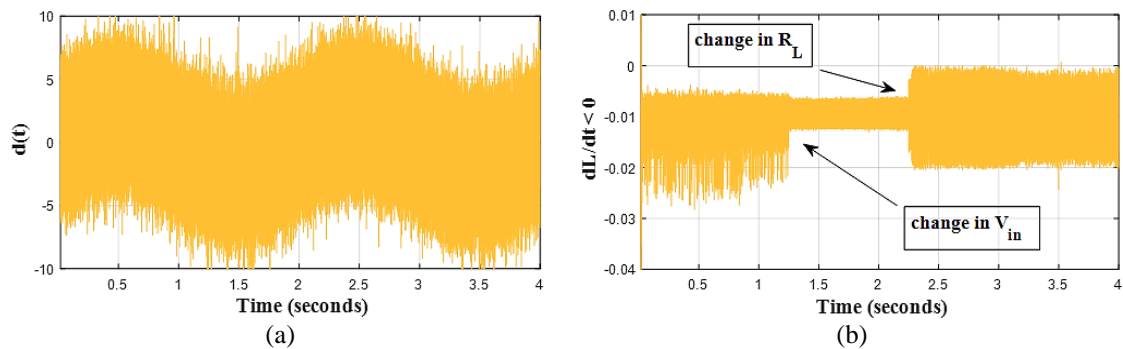(a) FSM control and (b) PI control

Figure 17. Response of the Lyapunov stability condition in the case of noise d(t) is fed: (a) random noise distribution $d(t)$ with amplitude ±10 V and (b) experimental performance $\frac{dL}{dt} = s^T \dot{s} \leq 0$

Similarly, to the simulation results, the experimental results demonstrated that the proposed FSMCS algorithm is significantly suitable for the DC-DC buck converter with high quality control performance, which includes low steady-state error, insignificant overshoot, and a high degree of compatibility of the measured voltage V_O and current I_L despite sudden changes in the source input, load, as well as the presence of noise. The improved control quality indexes are the rapid recovery time in the presence of varying parameters, compared to the classical PI controller. Table 4 presents a summary compatibility of the measured voltage V_O and current I_L using FSMCS compared to the classical PI control. The experimental statistics show that the FSMCS is more performance efficient with higher NRMSE coefficients.

Table 4. The experimental comparison of NRMSE coefficients

V_{in}, V_o^*, and R_L	FSMC	PI
V_{in} = 90 V	[95.72%, 90.99%]	[95.21%, 84.22%]
Change in V_{in}	[95.59%, 91.75%]	[94.91%, 78.06%]
Change in R_L	[94.15%, 93.75%]	[93.69%, 89.37%]
Change V_{in}, R_L	[93.89%, 94.00%]	[93.45%, 86.26%]
Change in d(t)	[93.94%, 94.20%]	[93.41%, 86.27%]

4. CONCLUSION

Since the control performance of buck converters is affected by uncertainties such as input voltage, resistance load, and noise, this paper proposes a sliding mode control strategy using a fuzzy observer to provide a higher sustainable performance. The control strategy includes two feedback loops in which a fuzzy supervisor is designed for the sliding surface to generate PWM pulses that have efficient duty cycles for the buck converter's switch to provide a stable, constant output voltage. To demonstrate the efficiency of the proposed FSMCS, the simulations and experiments were conducted in steady state and transient state by changing the source voltage V_{In}, setting voltage V_O^* and resistance load R_L as well as the presence of noise $d(t)$.

The simulated and experimental results have demonstrated that the proposed FSMCS algorithm is an advanced control method for the DC-DC buck converter in which the designed controller does not require a concrete mathematical model of the system, and the control law is implemented based on expert knowledge. The output voltage of the Buck converter has tracked various setting points despite sudden changes in load as well as in input voltage in the presence of noise. The output voltage of the buck converter has tracked various setting points despite sudden changes in load as well as in input voltage in the presence of noise. The compatibility index normalized root mean square error of the measured voltage and current using the FSMCS algorithm is [96.34% ± 1.02%, 95.09% ± 3.04%] higher than that using the PI algorithm which is [95.94% ± 3.01%, 85.72% ± 3.95%] in the presence of varying parameters. The overshoot percent of the current is decreased by about 16.7% ± 2.45% compared to using the PI algorithm. The improved control quality indicated that the proposed control strategy is significantly effective compared to the classical controllers in robustness control. However, the major disadvantage of this method is that the proposed fuzzy supervisor is not been generalized to various DC-DC buck converter systems. Future work is to extend the adaptation of this method to various converters over a larger operating range. Moreover, optimization algorithms will be applied to find appropriate parameters of the fuzzy models.

AUTHOR CONTRIBUTIONS STATEMENT

This journal uses the Contributor Roles Taxonomy (CRediT) to recognize individual author contributions, reduce authorship disputes, and facilitate collaboration.

Name of Author	C	M	So	Va	Fo	I	R	D	O	E	Vi	Su	P	Fu
Quan Vinh Nguyen	✓	✓	✓	✓			✓	✓	✓			✓	✓	✓
Huu-Toan Tran	✓			✓	✓	✓		✓	✓	✓	✓	✓	✓	
Long Thang Mai			✓		✓	✓	✓			✓	✓			

C : **C**onceptualization	I : **I**nvestigation		Vi : **Vi**sualization
M : **M**ethodology	R : **R**esources		Su : **Su**pervision
So : **So**ftware	D : **D**ata Curation		P : **P**roject administration
Va : **Va**lidation	O : Writing - **O**riginal Draft		Fu : **Fu**nding acquisition
Fo : **Fo**rmal analysis	E : Writing - Review & **E**diting		

CONFLICT OF INTEREST STATEMENT

Authors state no conflict of interest.

DATA AVAILABILITY

The data that support the findings of this study are available from the corresponding author, [HTT], upon reasonable request via email: tranhuutoan@iuh.edu.vn.

REFERENCES

[1]   H. Al-Baidhani, T. Salvatierra, R. Ordonez, and M. K. Kazimierczuk, "Simplified nonlinear voltage-mode control of PWM DC-DC buck converter," *IEEE Transactions on Energy Conversion*, vol. 36, no. 1, pp. 431–440, 2021, doi: 10.1109/TEC.2020.3007739.

[2]   J. M. Liu, P. Y. Wang, and T. H. Kuo, "A current-mode DC-DC buck converter with efficiency-optimized frequency control and reconfigurable compensation," *IEEE Transactions on Power Electronics*, vol. 27, no. 2, pp. 869–880, 2012, doi: 10.1109/TPEL.2011.2162079.

[3]   Y. Shen, Z. Qin, and H. Wang, "Modeling and control of DC-DC converters," *Control of Power Electronic Converters and Systems*, pp. 69–92, 2018, doi: 10.1016/B978-0-12-805245-7.00003-2.

[4]   P. Mattavelli, L. Rossetto, and G. Spiazzi, "Small-signal analysis of DC-DC converters with sliding mode control," *IEEE Transactions on Power Electronics*, vol. 12, no. 1, pp. 96–102, 1997, doi: 10.1109/63.554174.

[5]   C. K. Tse and K. M. Adams, "Quasi-linear modeling and control of DC-DC converters," *IEEE Transactions on Power Electronics*, vol. 7, no. 2, pp. 315–323, Apr. 1992, doi: 10.1109/63.136248.

[6]   N. F. Nanyan, M. A. Ahmad, and B. Hekimoğlu, "Optimal PID controller for the DC-DC buck converter using the improved sine cosine algorithm," *Results in Control and Optimization*, vol. 14, 2024, doi: 10.1016/j.rico.2023.100352.

[7]   S. M. Rakhtala and A. Casavola, "Real-time voltage control based on a cascaded super twisting algorithm structure for DC-DC converters," *IEEE Transactions on Industrial Electronics*, vol. 69, no. 1, pp. 633–641, 2022, doi: 10.1109/TIE.2021.3051551.

[8]   S. Dev and A. Ahmed, "A comparative analysis between H∞ and sliding mode controllers on automatic voltage regulator system," *PEEIACON 2024 - International Conference on Power, Electrical, Electronics and Industrial Applications*, pp. 278–282, 2024, doi: 10.1109/PEEIACON63629.2024.10800191.

[9]   W. Dong, S. Li, X. Fu, Z. Li, M. Fairbank, and Y. Gao, "Control of a buck DC/DC converter using approximate dynamic programming and artificial neural networks," *IEEE Transactions on Circuits and Systems I: Regular Papers*, vol. 68, no. 4, pp. 1760–1768, 2021, doi: 10.1109/TCSI.2021.3053468.

[10] A. Ahmed, N. P. Bishnu, and N. K. Roy, "A comparative analysis of intelligent algorithm-based tuning of PID controller for speed control of BLDC motor," in *2023 6th International Conference on Electrical Information and Communication Technology (EICT)*, IEEE, Dec. 2023, pp. 1–6, doi: 10.1109/EICT61409.2023.10427912.

[11] A. Heydari, "Optimal switching of DC-DC power converters using approximate dynamic programming," *IEEE Transactions on Neural Networks and Learning Systems*, vol. 29, no. 3, pp. 586–596, 2018, doi: 10.1109/TNNLS.2016.2635586.

[12] A. Ahmed and N. K. Roy, "Speed control of DC motor using sliding mode controller tuned by genetic algorithm," in *2023 10th IEEE International Conference on Power Systems (ICPS)*, IEEE, Dec. 2023, pp. 1–6, doi: 10.1109/ICPS60393.2023.10428866.

[13] A. Debnath, T. O. Olowu, S. Roy, I. Parvez, and A. Sarwat, "Particle swarm optimization-based PID controller design for DC-DC buck converter," in *2021 North American Power Symposium (NAPS)*, IEEE, Nov. 2021, pp. 1–6, doi: 10.1109/NAPS52732.2021.9654737.

[14] H. Guldemir, "Sliding mode speed control for DC drive systems," *Mathematical and Computational Applications*, vol. 8, no. 1–3, pp. 377–384, 2003, doi: 10.3390/mca8030377.

[15] Y. M. Alsmadi, V. Utkin, M. A. Haj-ahmed, and L. Xu, "Sliding mode control of power converters: DC/DC converters," *International Journal of Control*, vol. 91, no. 11, pp. 2472–2493, 2018, doi: 10.1080/00207179.2017.1306112.

[16] M. A. F. Al-Qaisi, M. A. Shehab, A. Al-Gizi, and M. Al-Saadi, "High performance DC/DC buck converter using sliding mode controller," *International Journal of Power Electronics and Drive Systems*, vol. 10, no. 4, pp. 1806–1814, 2019, doi: 10.11591/ijpeds.v10.i4.pp1806-1814.

[17] D. Ravikumar and G. K. Srinivasan, "Implementation of higher order sliding mode control of DC–DC buck converter fed permanent magnet DC motor with improved performance," *Automatika*, vol. 64, no. 1, pp. 162–177, 2023, doi: 10.1080/00051144.2022.2119499.

[18] A. Ahmed, N. K. Roy, and A. Nasir, "A novel weighted exponential sliding mode controller with a modified reaching law for the frequency regulation of a renewable integrated isolated AC microgrid," *Electric Power Systems Research*, vol. 237, p. 111027, Dec. 2024, doi: 10.1016/j.epsr.2024.111027.

[19] N. P. Bishnu, Z. Bin Azam, A. Ahmed, and N. K. Roy, "Robust automatic voltage regulation using modified super twisting sliding mode control," in *2024 IEEE International Conference on Power, Electrical, Electronics and Industrial Applications (PEEIACON)*, IEEE, Sep. 2024, pp. 260–265, doi: 10.1109/PEEIACON63629.2024.10800567.

[20] A. Ahmed, N. K. Roy, and K. Mahmud, "Achieving robust and optimal speed control of dc motor through sliding mode control tuned by genetic and particle swarm optimization algorithms," *Smart Grids and Sustainable Energy*, vol. 9, no. 2, 2024, doi: 10.1007/s40866-024-00223-3.

[21] J. H. Lilly, *Fuzzy Control and Identification*. Wiley, 2010. doi: 10.1002/9780470874240.

[22] R. Isermann, "On fuzzy logic applications for automatic control, supervision, and fault diagnosis," *IEEE Transactions on Systems, Man, and Cybernetics Part A: Systems and Humans.*, vol. 28, no. 2, pp. 221–235, 1998, doi: 10.1109/3468.661149.

[23] J. M. D. C. Sousa and U. Kaymak, "Model predictive control using fuzzy decision functions," *IEEE Transactions on Systems, Man, and Cybernetics, Part B: Cybernetics*, vol. 31, no. 1, pp. 54–65, 2001, doi: 10.1109/3477.907564.

[24] O. Aissa, R. Benkercha, Z. Bouchama, B. Babes, and I. Colak, "Experimental assessment of fuzzy-tree adaptive synergetic control law for DC/DC buck converter," *Soft Computing*, vol. 28, no. 20, pp. 12191–12205, Oct. 2024, doi: 10.1007/s00500-024-09916-4.

[25] S. M. Ghamari, H. G. Narm, and H. Mollaee, "Fractional-order fuzzy PID controller design on buck converter with antlion optimization algorithm," *IET Control Theory and Applications*, vol. 16, no. 3, pp. 340–352, 2022, doi: 10.1049/cth2.12230.

[26] M. B. Ghalia and A. T. Alouani, "Sliding mode control synthesis using fuzzy logic," in *Proceedings of 1995 American Control Conference - ACC'95*, American Autom Control Council, 1995, pp. 1528–1532, doi: 10.1109/ACC.1995.521007.

[27] K. N. Swamy, P. H. Prithvi, and N. S. K. Chakravarthi, "Design buck converter using fuzzy logic controller," *International Journal for Modern Trends in Science and Technology*, vol. 5, no. 10, 2019.

[28] E. Radwan, M. Nour, E. Awada, and A. Baniyounes, "Fuzzy logic control for low-voltage ride-through single-phase grid-connected PV inverter," *Energies*, vol. 12, no. 24, p. 4796, Dec. 2019, doi: 10.3390/en12244796.

[29] Z. B. Duranay, H. Guldemir, and S. Tuncer, "Fuzzy sliding mode control of DC-DC boost converter," *Engineering, Technology & Applied Science Research*, vol. 8, no. 3, pp. 3054–3059, 2018, doi: 10.48084/etasr.2116.

[30] M. Leso, J. Zilkova, and P. Girovsky, "Development of a simple fuzzy logic controller for DC-DC converter," in *2018 IEEE 18th International Power Electronics and Motion Control Conference (PEMC)*, IEEE, Aug. 2018, pp. 86–93, doi: 10.1109/EPEPEMC.2018.8521896.

[31] K. Bendaoud *et al.*, "Fuzzy logic controller (FLC): Application to control DC-DC buck converter," in *2017 International Conference on Engineering & MIS (ICEMIS)*, IEEE, May 2017, pp. 1–5, doi: 10.1109/ICEMIS.2017.8272980.

[32] N. D. Bhat, D. B. Kanse, S. D. Patil, and S. D. Pawar, "DC/DC buck converter using fuzzy logic controller," in *2020 5th International Conference on Communication and Electronics Systems (ICCES)*, IEEE, Jun. 2020, pp. 182–187, doi: 10.1109/ICCES48766.2020.9138084.

[33] U. S. Sangeeth and N. K. Arun, "Fuzzy logic control of DC-DC buck converter in DC distribution system with constant power load," in *Proceedings of the International Conference on Artificial Intelligence Techniques for Electrical Engineering Systems (AITEES 2022)*, 2023, pp. 180–191, doi: 10.2991/978-94-6463-074-9_16.

BIOGRAPHIES OF AUTHORS

Quan Vinh Nguyen [iD] [g] [SC] [C] received the M.S. degree in Automation technology Ho Chi Minh City University of Technology (HCMUT), Vietnam, in 2011, and the Ph.D. degree in electrical engineering from HCMUT, Vietnam, in 2020. He is currently employed at the Faculty of Electronics Technology, Industrial University of Ho Chi Minh City, Vietnam. His research interests are circuit design, power electronics and automatic control. He can be contacted at email: quan_01037027@iuh.edu.vn.

Huu-Toan Tran [iD] [g] [SC] [C] is a senior lecturer in Faculty of Electronic Technology, Industrial University of Ho Chi Minh City, Vietnam since 2008; and he has been the head of department of Intelligence System. He received the M.S. degree in Automation from Ho Chi Minh City University of Technology in 2009, and the Ph.D. degree in Electronic Science and Technology from University of Electronic Science and Technology of China in 2015. His research interests include intelligence and application control, wearable robot, and human-robot interaction. He can be contacted at email: tranhuutoan@iuh.edu.vn.

Long Thang Mai [iD] [g] [SC] [C] received the B.S. and M.S. degrees in Automatic control from Viet Nam National University, Ho Chi Minh City University of Technology, Viet Nam in 2004 and 2009, respectively, and then received the Ph.D. degree in Control science and engineering from Hunan University, China in 2014. He has been a lecturer at Industrial University of Ho Chi Minh City, Viet Nam since 2009. His current research interests include robotic control, learning control and intelligent control. He can be contacted at email: maithanglong@iuh.edu.vn.